Bioelectrochemistry 140 (2021) 107831

Contents lists available at ScienceDirect

Bioelectrochemistry

journal homepage: www.elsevier.com/locate/bioelechem

Mutational burden, MHC-I expression and immune infiltration as limiting factors for *in situ* vaccination by TNFα and IL-12 gene electrotransfer

Urska Kamensek [a,b,*], Katja Ursic [a,b], Bostjan Markelc [a,c], Maja Cemazar [a,d], Vita Setrajcic Dragos [e], Gregor Sersa [a,c]

[a] Department of Experimental Oncology, Institute of Oncology Ljubljana, Zaloska cesta 2, SI-1000 Ljubljana, Slovenia
[b] University of Ljubljana, Biotechnical Faculty, Jamnikarjeva ulica 101, SI-1000 Ljubljana, Slovenia
[c] Faculty of Health Sciences, University of Ljubljana, Zdravstvena pot 5, SI-1000 Ljubljana, Slovenia
[d] Faculty of Health Sciences, University of Primorska, Polje 42, SI-6310 Izola, Slovenia
[e] Department of Molecular Diagnostics, Institute of Oncology Ljubljana, Zaloska cesta 2, SI-1000 Ljubljana, Slovenia

ARTICLE INFO

Article history:
Received 31 December 2020
Received in revised form 21 April 2021
Accepted 23 April 2021
Available online 28 April 2021

Keywords:
In situ vaccination
Gene electrotransfer
Interleukin 12
Tumor necrosis factor-α
TS/A
Tumor mutational burden

ABSTRACT

In situ vaccination is a promising immunotherapeutic approach, where various local ablative therapies are used to induce an immune response against tumor antigens that are released from the therapy-killed tumor cells. We recently proposed using intratumoral gene electrotransfer for concomitant transfection of a cytotoxic cytokine tumor necrosis factor-α (TNFα) to induce *in situ* vaccination, and an immunostimulatory cytokine interleukin 12 (IL-12) to boost the primed immune response. Here, our aim was to test the local and systemic effectiveness of the approach in tree syngeneic mouse tumor models and associate it with tumor immune profiles, characterized by tumor mutational burden, immune infiltration and expression of PD-L1 and MHC-I on tumor cells. While none of the tested characteristic proved predictive for local effectiveness, high tumor mutational burden, immune infiltration and MHC-I expression were associated with higher abscopal effectiveness. Hence, we have confirmed that both the abundance and presentation of tumor antigens as well as the absence of immunosuppressive mechanisms are important for effective *in situ* vaccination. These findings provide important indications for future development of *in situ* vaccination based treatments, and for the selection of tumor types that will most likely benefit from it.

1. Introduction

Cancer is a diverse group of systemic diseases caused by mutations that have in common immune system malfunctions, since immune cells fail to recognize or fight the disease. Different immunotherapies aim to restore the anticancer immunity by exploiting the patient's own adaptive immune system. One of the more robust immunotherapeutic approaches is the so-called *in situ* vaccination, where various local ablative therapies are used to induce a specific immune response against tumor's own antigens that are released from the therapy-killed tumor cells [1,2]. However, according to the clinical experience, to achieve a systemic and durable response, these therapies need to be combined with immune adjuvants that stimulate the immune system [3–5].

In our group, we are exploiting a form of non-viral gene therapy called gene electrotransfer (GET) that can be used both, to induce *in situ* vaccination, and also to stimulate the immune response. Using GET approach, genetic material encoded on plasmid vectors can be transferred directly to targeted tissue where electric pulses are applied [6,7]. Transferred genetic material is then expressed locally, making GET especially promising for delivering different cytokines, which are toxic if administered systemically [8].

In our previous study, we have used intratumoral GET of two cytokines: tumor necrosis factor-α (TNFα) and interleukin-12 (IL-12) [9]. In the published study, TNFα GET was intended as a local ablative therapy priming the *in situ* vaccination, and IL-12 GET as an immunological adjuvant boosting the induced immune response against the released tumor antigens. The results confirmed the feasibility of the approach as both cytokines were

* Corresponding author at: Urska Kamensek, Department of Experimental Oncology, Institute of Oncology Ljubljana, Zaloska cesta 2, SI-1000 Ljubljana, Slovenia.
E-mail address: ukamensek@onko-i.si (U. Kamensek).

https://doi.org/10.1016/j.bioelechem.2021.107831
1567-5394/

expressed after concomitant GET of the two plasmids. Furthermore effectiveness of the approach in eliciting a potent and durable anti-tumor response in a mouse melanoma B16-F10 tumor model was demonstrated. However, we didn't directly prove the systemic effectiveness of the therapy, such as the abscopal effect.

Hence, in the current study we wanted to determine the effectiveness of concomitant intratumoral TNFα and IL-12 gene electrotransfer in eliciting an abscopal effect. Furthermore, we chose to test the approach in additional tumor models. Namely, *in situ* vaccination theoretically has the potential to be effective in different cancer types, since it harnesses the patient's own immune system and tumor's own antigens. Conversely, the sporadic results achieved with various immunotherapeutic approaches in patients, highlight the significance of the characteristics, like tumor immune profile and tumor mutational burden (TMB), for the treatment outcome [10]. Therefore, for this study, we selected three syngeneic experimental tumor models as surrogates for tumor-immune profiles find in human cancers [11]. The first two were well-characterized mouse tumor models B16-F10 melanoma and CT26 colon carcinoma [12–14]. For the third one, we decided on TS/A mammary adenocarcinoma tumor model, which is used in numerous immunotherapy studies but has not been fully evaluated before in regard to its immune status and TMB [15].

Using the selected three tumor models, the aim of this study was to associate the local and abscopal therapeutic effectiveness of *in situ* vaccination by TNFα and IL-12 GET with the tumor immune profiles characterized by TMB, immune cell infiltration, and expression of PD-L1 and MHC-I on tumor cells.

2. Materials and methods

2.1. Plasmids

TNFα was encoded in pORF9 mTNFα plasmid (Invivogen, Toulouse, France) and IL-12 in our custom-made plasmid pCol-mIL-12-ORT [16]. The plasmids were isolated using the EndoFree Plasmid Mega Kit (Qiangen, Hilden, Germany) and diluted in endotoxin-free water (Qiagen) to a concentration of 1 or 2 mg/mL. Plasmid concentrations were determined spectrophotometrically (Epoch Microplate Spectrophotometer, Take3™ Micro-Volume Plate, BioTek, Bad Friedrichshall, Germany). Additionally, plasmids quality was confirmed by 260/280 ratio and by restriction analysis.

2.2. Cells, animals and tumor models

TS/A mammary adenocarcinoma cells [17] (authenticated by CellCheck (mouse STR profile and interspecies contamination test), IDEXX BioAnalytics, Westbrook, ME, USA) and B16-F10 malignant melanoma cells (American Type Culture Collection) were cultured in Dulbecco's Modified Eagle Medium (DMEM, Gibco, Thermo Fischer Scientific, Waltham, MA, USA), and CT26 colorectal carcinoma cells (American Type Culture Collection) in Roswell Park Memorial Institute (RPMI) 1640 Medium (Gibco, Thermo Fischer Scientific), both supplemented with 5% fetal bovine serum (Thermo Fischer Scientific), 10 mM L-glutamine (GlutaMAX, Thermo Fischer Scientific), 100 U/ml penicillin (Grünenthal, Aachen, Germany) and 50 mg/ml gentamicin (Krka, Novo Mesto, Slovenia) in a 5% CO_2 humidified incubator at 37 °C. Cells were tested every 3 months for mycoplasma with MycoAlert™ PLUS Mycoplasma Detection kit (Lonza, Basel, Switzerland) and found negative.

Six- to eight-weeks old female BALB/cAnNCrl mice, syngeneic for TS/A and CT26 tumor models, and C57Bl/6NCrl mice, syngeneic for B16-F10 tumor model, were purchased from Charles River Laboratories Italia (Calco, Italy). Mice were kept in a specific pathogen-free colony at a constant room temperature with a 12 h light/dark cycle, and provided with food and water *ad libitum*. Animal experiments were performed in compliance with the official guidelines of EU Directive 2010/63/EU, ARRIVE guidelines, and with permission from the Veterinary Administration of the Ministry of Agriculture, Forestry and Food of the Republic of Slovenia (permission no. U34401-1/2015/43) that was approved by the National Ethics Committee for Experiments on Laboratory Animals.

Tumors were induced by a subcutaneous injection of cell suspension in 0.1 ml of saline solution into the shaved flanks of syngeneic mice. TS/A tumors were established by injection of 2×10^6 of TS/A cells, and CT26 tumors by injection 0.5×10^6 of CT26 cells. Dual flank tumor models were established by subcutaneous injection of 1×10^6 of B16-F10, 0.5 of CT 26×10^6 and 2×10^6 of TS/A cells in the right flank of syngeneic mice followed, 3 day later, by the subcutaneous injection of a reduced amount of cells (80%) in the left flank of the mice. The protocol for dual flank tumor model was optimized so that right tumors in all tree tumor models reached the size of 40 mm^3 (*i.e.* 6 mm in the longest diameter) in one-week time, and at the same time, left tumors were already palpable. The size of 40 mm^3 was chosen to be comparable with studies in single tumor models and also immune profiling was done on 40 mm^3 tumors.

After approximately one week, when tumors (the right tumors in the dual flank tumor model) reached 40 mm^3, mice were randomly divided into different treatment groups consisting of 8–10 animals per group. In the dual flank tumor models, the right tumor was regarded as a primary tumor and was treated, and the left tumor was regarded as a metastasis and was left untreated. During the treatments, mice were anesthetized by isoflurane gas anesthesia (Chiesi, Parma, Italy). Throughout the experiments, the weight of the mice was monitored as a general index of well-being. A tumor volume of app. 300 mm^3 or the loss of 15% of the body mass were pre-set humane endpoint of the experiments.

2.3. Tumor immune status

Tumor-immune profiling was done by flow cytometry analysis of single cell suspensions prepared from B16-F10, CT26 or TS/A tumor tissue. When tumors reached a volume of 40 mm^3 mice were sacrificed and tumors excised, dissected into smaller fragments and subjected to enzymatic digestion in Hanks' Balanced Salt solution (with Calcium and Magnesium; GIBCO) containing 2 mg/mL of collagenase type 2 (Worthington Biochem) and 2 U/mL DNase I (Thermo Fisher Scientific) for 45 min with gentle shaking at 37 °C. The digested tumor suspension was then strained through 50 μm strainers (Sysmex, Kobe, Japan) to get single cell suspensions, centrifuged (5 min, 4 °C, 400 g) and washed in PBS. A total of 2×10^6 cells were first incubated with TruStain FcX (Biolegend, San Diego, CA, USA) for 5 min on ice to block non-specific binding of immunoglobulin to the Fc receptors. Cell were then stained with a defined antibody panel containing Fixable Viability Dye eFluor™ 780, anti-PD-L1 PE, anti- MHC-I APC (H-2Kd for CT26 and TS/A tumors and H-2 Kb for B16-F10 tumors), anti-CD45 Alexa Fluor 700, anti-CD8 Alexa Fluor 488, anti-CD4 PerCp-Cyanine 5.5 (all Thermo Fisher Scientific) and anti-CD3 Brilliant Violet 510 (Biolegend) labeling antibodies for 30 min on ice (Supplementary Table S1). After incubation, cells were washed twice with PBS and resuspended in IC Fixation buffer (Thermo Fisher Scientific). Stained cell suspensions were analyzed with FACSCanto II flow cytometer (BD Biosciences). The gating strategy was determined by FMOs or isotype controls (Supplementary Fig. S2). Data were analyzed using FlowJo software (Tree Star Inc., Ashland, OR, USA).

2.4. Tumor mutational burden

For whole-exome sequencing (WES), DNA was extracted from TS/A cells pellet (*in vitro* culture) and BALB/c mouse tail tissue using DNeasy Blood and Tissue Kit with RNAse A (Qiagen). Concentration was determined by Qubit dsDNA broad-range (BR) assay (Thermo Fisher Scientific) on Qubit 4 Fluorimeter (Thermo Fisher Scientific). Quality and purity (OD 260/280) were ensured by spectrophotometric analysis (Epoch Microplate Spectrophotometer, Take3™ Micro-Volume Plate, BioTek, Bad Friedrichshall, Germany). Whole-exome sequencing (WES) and analysis was performed at GeneWiz (South Plainfield, NJ, US). The enrichment of exonic regions was done using the SureSelect XT Mouse All Exon Kit (Agilent) followed by Illumina HiSeq 2 × 150 paired-end sequencing. Alignment to *Mus musculus* mm9 reference genome and variant calling was performed using Edico Genome's Dragen pipeline. SNVs and small INDELs were annotated using UCSC Variant Annotation Integrator (VAI). UCSC canonical transcripts were selected for variant description. All variants present in less than 1% allele fraction were considered sequencing artifacts and were filtered out. Additional variant filtering was performed to remove known common variants (known population level SNPs) using the VAI package against dbSNP (v128), because a modern BALB/c mouse DNA was used as a germline and not the exact mouse from which the TS/A tumor cell line was generated in 1983. Tumor-normal analysis was performed by subtracting variants identified from BALB/c DNA from variants identified in the TS/A cell line (Supplementary MS Excel spreadsheet S3). Tumor mutational burden was expressed as the number of somatic synonymous and non-synonymous variants located within coding regions (SNVs, Indels). Literature data were used for CT26 and B16-F10 mutational burden [18].

2.5. Gene electrotransfer (GET)

GET was performed on 40 mm^3 tumors by intratumoral injection of 50 μL of plasmid solution containing 50 μg of each plasmid, followed 5 min later, by application of 8 (4 + 4 in perpendicular directions) electric pulses (plate electrodes, 600 V/cm, 5 ms, 1 Hz) by Electro Cell B10 electric pulse generator (Leroy Biotech, St-Orens-de-Gameville, France). Good contact between the tumor and the electrodes was ensured by a conductive gel (Ultragel, Budapest, Hungary). In the groups receiving IL-12 GET either in combination with TNFα GET or alone, IL-12 GET was repeated 6 days after the first GET. In the control group (CTRL), mice were injected with 50 μL of endotoxin-free water. The tested therapeutic groups were as follows: TNF: GET of the TNFα plasmid, IL-12: GET of the IL-12 plasmid repeated twice with an interval of 6 days, TNF + IL-12: concomitant GET of the TNFα and IL-12 plasmids, followed 6 days later by GET of the IL-12 plasmid and CTRL: control group. To comply with the 3R rule, EP only group and control plasmid groups were not included in these experiments since these groups were tested in previous experiments by our group [9,19,20]

2.6. Therapeutic effectiveness

Tumor growth of both the treated and the untreated tumors was determined by measuring the tumors every 2–3 days using digital Vernier caliper. Tumor volume was calculated by the formula: $V = a \times b \times c \times \pi/6$; where a, b, and c correspond to the three orthogonal diameters of the tumor. From the tumor volumes, arithmetic means (AM) for each group were calculated, and tumor growth curves were drawn with error bars representing the standard error of the mean (SEM). Times when tumors reached 100 mm^3 (t_{100}) or 50 mm^3 (t_{50}) for the untreated tumors in the dual flank tumor model, were interpolated from the growth curves. To compensate for the different tumor growth kinetics in the tree tumor models, statistical analysis was done on tumor growth delay data that was normalized to the tumor growth of pertinent control tumors. Specifically, for the treated tumors, tumor growth delay (TGD_{100}) was calculated as the difference in t_{100} of the treated tumors (t_{100}exp) compared to control tumors (t_{100}ctrl): $TGD_{100} = t_{100}exp - \bar{t}_{100}$ ctrl. For the untreated tumors in the dual flank model, the calculation of TGD was based on the time when untreated tumors reached 50 mm^3: $TGD_{50} = t_{50}exp - \bar{t}_{50}$ ctrl. Additionally, Pearson correlation coefficient between the growth of the treated and the corresponding untreated tumor in the same animal on day 8 was calculated.

2.7. Statistical analysis

GraphPad Prism version 8.1.2. (GraphPad Software, San Diego, CA, USA) was used for data analysis and graphical presentations. The Shapiro–Wilk test was performed to test for data normality. Normally distributed data were presented as the mean ± standard error or mean (SEM). Non-normally distributed data were presented as the median with data range (min, max). Normally distributed data with equal variance were analyzed with a one-way ANOVA, followed by Tukey's test for multiple comparisons. Normally distributed data with unequal variance were analyzed with a Browne–Forysthe and Welch's ANOVA, followed by Dunnet's T3 test for multiple comparisons. Non-normally distributed data were analyzed with a Kruskal–Wallis ANOVA on Ranks, followed by Dunn's test for multiple comparisons. Pearson correlation test was used to measure the direction and strength of correlations. A significant difference between experimental groups was defined at $p < 0.05$.

3. Results

3.1. Immune profile

Immune profiling was performed on tumors when they reached the appropriate size for the treatment (40 mm^3). No differences between tumor models were determined in CD45+ (Fig. 1 a) and CD3+ infiltration (Fig. 1 b), however the percentage of CD4+ helper T cells (Fig. 1 c) and CD8+ cytotoxic T cells (Fig. 1 d) was the highest in CT26 tumor model. The sum CD8+ and CD4+ cell was statistically higher in CT26 tumors (44%) compared to B16-F10 (15%) and TS/A (3.9%) tumors (Fig. 1 e). More than half of tumor cells were PD-L1 positive in all tree tumor models, without any statistically significant difference between them (Fig. 1 e). B16-F10 tumors were mostly MHC-I negative (only 7.4% of MHC-I positive cells), while most (96%) tumor cells were MHC-I positive in CT26 and 69% in TS/A tumor model (Fig. 1 f).

3.2. Mutational burden

Mutational burden of TS/A cell line was determined by WES analysis that identified 712 synonymous and non-synonymous single nucleotide variants (SNVs) in exons, of which 46 were found in untranslated regions (UTR) and 666 in coding sequences (CDS). Among CDSs, 137 mutation were determined as synonymous or silent and 529 as non-synonymous, corresponding to mutational rate of 16.5 mutations per Mb (assuming 32 Mb of protein-coding sequence). Additionally, 33 short insertions and deletions (indels) were identified in exons (Table 1). Mutational burden of TS/A was compared to the mutational burden of CT26 and B16-F10 tumor models obtained from the literature [13], which rendered TS/A tumor model with 712 SNPs the least mutated compared to CT26 with 3023 SNPs and B16-F10 with 908 SNPs.

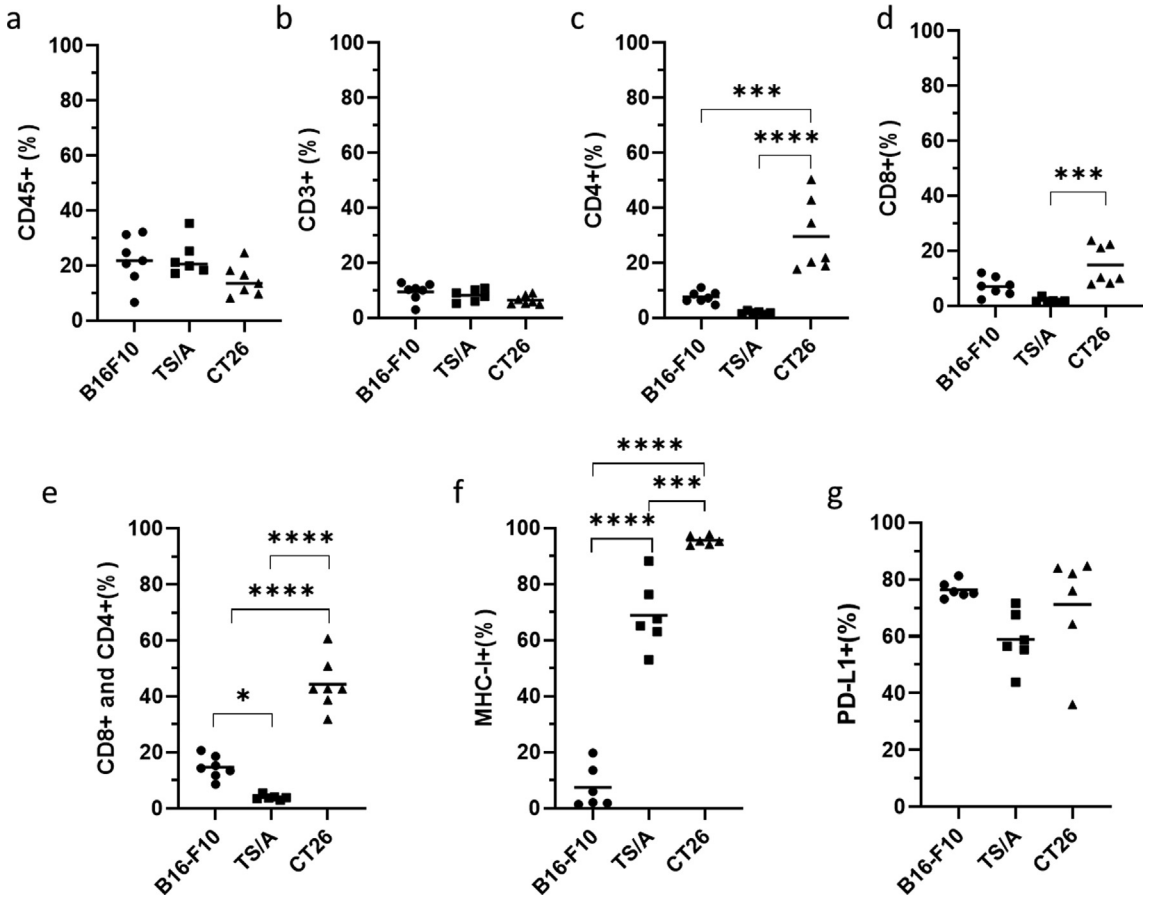

Fig 1. Immune profiles of B16-F10, TS/A and CT26 tumors before treatment. Percentage of (a) CD45+, (b) CD3+, (c) CD4+ helper T cells, (d) CD8+ cytotoxic T cells and (e) sum of CD4+ and CD8+ immune cells. Percentage of (f) MHC-I and (g) PD-L1 positive tumor cells. n = 6 animals/group, individual values with mean. (*) $P \leq 0.05$, (**) $P \leq 0.01$, (***) $P \leq 0.001$, (****) $P \leq 0.0001$.

Table 1
TS/A tumor mutational burden determined by WES analysis.

	Single nucleotide variants	Indels
Number of mutations	712	33
in exons	712	33
in UTRs	46	6
in CDSs	666	27
synonymous	137	/
non-synonymous	529 = 16.5/Mb	27
missense	507	/
premature stop	20	27
stop loss	2	/

(UTRs) untranslated regions, (CDSs) coding sequences, (Indels) insertions and deletions.

3.3. Local effectiveness

Local effectiveness of TNFα and IL-12 GET was tested in TS/A and CT26 tumor models. The concomitant GET was more effective than TNFα and IL-12 GET monotherapies in both tumor models (Fig. 2 a, b). The TGD_{100} was 16 days in CT26 tumors and 13 days in TS/A tumors (Supplementary table S4). In TS/A tumor model both TNFα and IL-12 GET monotherapies contributed equally to the effectiveness of combined GET (TGD_{100} was 5 and 6 days respectively), while in CT26, IL-12 GET was more effective (TGD_{100} was 8 days) than TNFα GET (TGD_{100} was 5 days). In the CT26 tumor model, t_{100} after concomitant GET and both monotherapies was significantly longer compared to control group, while in TS/A only the combined treatment resulted in significantly prolonged t_{100}. (Fig. 2 c, d). There were no complete responses.

3.4. Abscopal effectiveness

The abscopal effectiveness of the concomitant TNFα and IL-12 GET was tested in B16-F10, CT26 and TS/A dual flank tumor models. The TGD_{50} for untreated tumors was 9 days in CT26 tumor model compared to only 1 day in B16-F10 tumors and 0 days in the TS/A tumor model (Supplementary table S4). In the CT26 tumor model, t_{50} after concomitant GET, but not after monotherapies, was significantly longer compared to control group (Fig. 3 a - f). Additionally, in this tumor model, correlation in growth of treated and untreated tumors was positive and statistically significant after both monotherapies and after concomitant GET (Supplementary table S5, Fig. 3 j - l). Due to the burden of the second tumor in dual flank tumor model, t_{100} was not reached in all tumors, therefore TGD_{100} could not be calculated for the primary tumors (Fig. g - i).

3.5. Association of therapeutic effectiveness with tumor immune profiles

Tumor growth data retrieved from the current and our previous study (local effectiveness in B16 F10 tumor model [9]) were combined to draw summarizing graphs for local and abscopal effectiveness of concomitant IL-12 and TNF GET for all tree tumor models. Next, both local and abscopal antitumor effectiveness were plotted

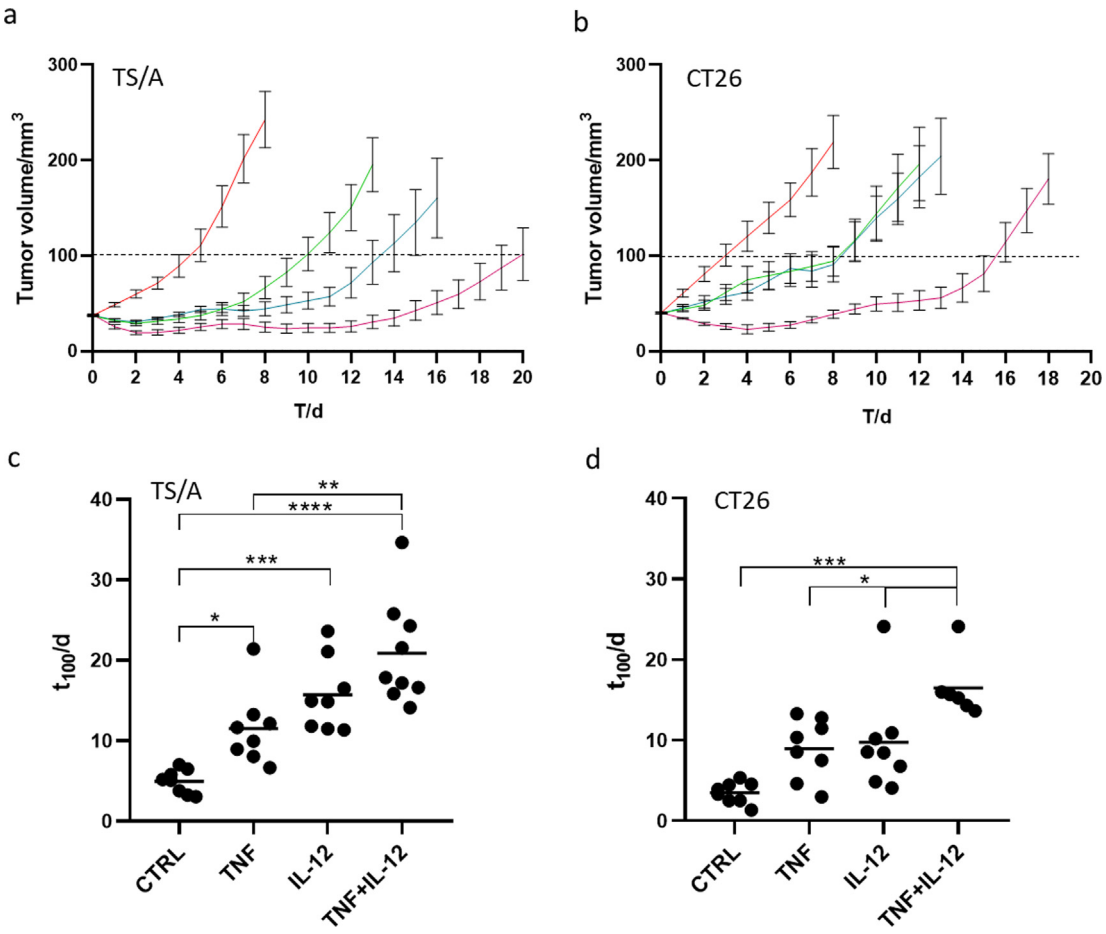

Fig 2. Local therapeutic effectiveness of concomitant TNFα and IL-12 GET in CT26 and TS/A (single) tumor models: Tumor growth of treated (a) CT26 and (b) TS/A tumors. Times when (c) CT26 and (d) TS/A tumors reached 100 mm^3 (t_{100}). (—) control group, (—) TNFα GET monotherapy, (—) IL-12 GET monotherapy, (—) concomitant TNFα and IL-12 GET, (GET) gene electrotransfer. n = 8–9 animals/group, tumor growth curves drawn as mean tumor volume with standard error of mean, t_{100} drawn as individual values with mean. (*) $P \leq 0.05$, (**) $P \leq 0.01$, (***) $P \leq 0.001$, (****) $P \leq 0.0001$.

against selected immunological parameters: *i.e.* TMB (for CT26 and B16-F10 TMB data was retrieved from literature [18]), immune infiltration (the sum of CD8+ and CD4+ cells), PD-L1 and MHC-I expression on tumor cells (Fig. 4b - e, Fig. 4 g - j). This graphic representation allowed us to identify critical immunological parameters that affect treatment's local and abscopal effectiveness. Local effectiveness was statistically significantly higher in B16-F10 tumor model compared to TS/A and CT26 tumor models (Fig. 4 a), while abscopal effectiveness was statistically significantly higher in CT26 tumor model compared to B16-F10 and TS/A (Fig. 4 f). No correlation was detected for local effectiveness for any of the immunological parameters (Fig. 4 b-e), while higher TMB (Fig. 4 g) and the tumor infiltration with CD4+ and CD8+ cells (Fig. 4 h) correlated with higher abscopal effectiveness (Supplementary table S6). Higher abscopal effectiveness was also associated with higher MHC-I expression on tumor cells (Fig. 4 j), although not statistically significantly, while PDL-1 expression (Fig. 4 i) did not correlate with abscopal effectiveness.

4. Discussion

GET is an excellent method for localized *in vivo* transfection, allowing simultaneous transfection of multiple plasmids. Our previous work has established that concomitant intratumoral electrotransfer of TNFα and IL-12 plasmids is effective in eliciting a potent and durable antitumor response in murine melanoma model, confirming the relevance of this gene therapy based approach for *in situ* vaccination [9]. The present study in three immunologically different mouse syngeneic tumor models shows that systemic effectiveness of the approach very much depends on the tumor's immune status: High TMB, immune infiltration and MHC-I expression proved to be important for abscopal effectiveness, while none of the tested immune characteristic proved to be predictive for local effectiveness.

The three tumor models used in the study were selected to represent diverse immune profiles seen in human cancers. We decided for B16-F10 melanoma, CT26 colorectal carcinoma and TS/A mammary adenocarcinoma. B16-F10 is a cytokine deficient and MHC-I suppressed tumor model [21,22], which makes it invisible for immune system and therefore not highly infiltrated with immune cells. Hence, in spite of its moderately high mutational burden [13], it is often classified as a immunologically cold tumor. Low infiltration and MHC-I expression in B16-F10 tumors was also confirmed in our study. The CT26 tumor model, on the other hand, is considered an immunologically hot tumor, with high mutational burden and infiltration of immune cells [13,14], which is also in line with our findings. Our third tumor model was TS/A mammary adenocarcinoma that has been used in numerous immunotherapy studies [15,23,24]. Although, TS/A has not been systematically evaluated regarding its immune status and TMB, it is typically described as poorly immunogenic [15,25]. The results of our immune profiling demonstrated that TS/A has a relatively high MHC-I expression

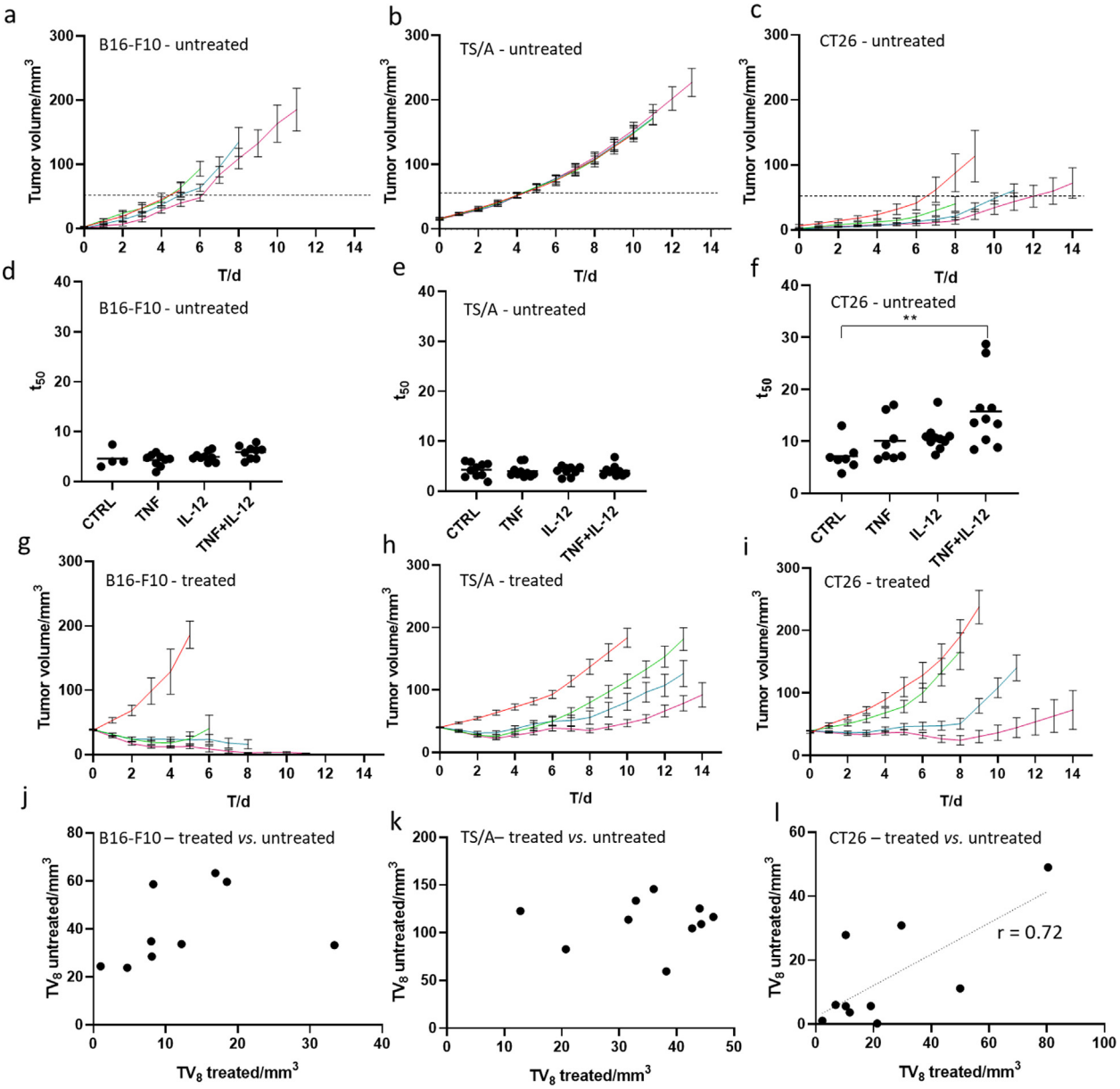

Fig 3. Abscopal therapeutic effectiveness of concomitant TNFα and IL-12 GET in B16-F10, CT26 and TS/A dual flank tumor models: Tumor growth of untreated (a) B16-F10, (b) TS/A and (c) CT26 tumors. Times when untreated (d) B16-F10, (e) TS/A and (f) CT26 tumors reached volume of 50 mm^3 (t_{50}). Tumor growth of treated (g) B16-F10, (h) TS/A and (i) CT26 tumors. Correlation in size of treated and untreated (j) B16-F10, (k) TS/A and (l) CT26 tumors in the same animal. n = 9–10 animals/group, tumor growth curves drawn as mean tumor volume with standard error of mean, t_{50} drawn as individual values with mean. Correlations drown as individual values for treated tumor volume plotted against untreated tumor volume in the same animal on day 8 after the treatment. Simple linear regression line indicates statistically significant correlation (r = 0.72). (—) control group, (—) TNFα GET monotherapy, (—) IL-12 GET monotherapy, (—) concomitant TNFα and IL-12 GET, (GET) gene electrotransfer, (TV_8) tumor volume on day 8. (**) $P \leq 0.01$.

and is not highly infiltrated with CD4+ or CD8+ immune cells, which is in line with a cold tumor.

Since TS/A cell line has not been sequenced before, we opted to determine its TMB, which proved quite difficult due to the discrepancies in the definition and reporting of TMB. Usually, TMB is defined as a number of nonsynonymous mutations in a tumors exome [26]. However reporting all mutations could be a more relevant indicator of tumors foreignness [27]. Although the reported TMB can vary substantially based on the analysis used [28,29], the consensus is that CT26 tumors are highly mutated with 2000–3500 SNVs and B16-F10 moderately with 1000–2000 SNVs [12,18]. Using an analysis comparable to that used in Castle et al. [13], we identified 712 SNVs in the TS/A tumors compared to the naïve BALB/c mouse genome, making it the least mutated among the tumor models used in our study.

After determining the pretreatment immune profiles of the selected tumor modes, we tested the local and abscopal effectiveness of the concomitant TNFα and IL-12 GET. In the previous study, we proved that our approach is a locally effective treatment in B16-F10 tumor model with almost 80% of complete responses [9]. Moreover, the relevance of the approach for *in situ* vaccination was confirmed by its ability to elicit a potent and durable antitumor response, indicated by the expansion of effector immune cells in the lymph nodes, resistance of cured mice to secondary challenge with tumor cells and vitiligo like depigmentation of fur at the site of cured tumors. Results of the present study show that

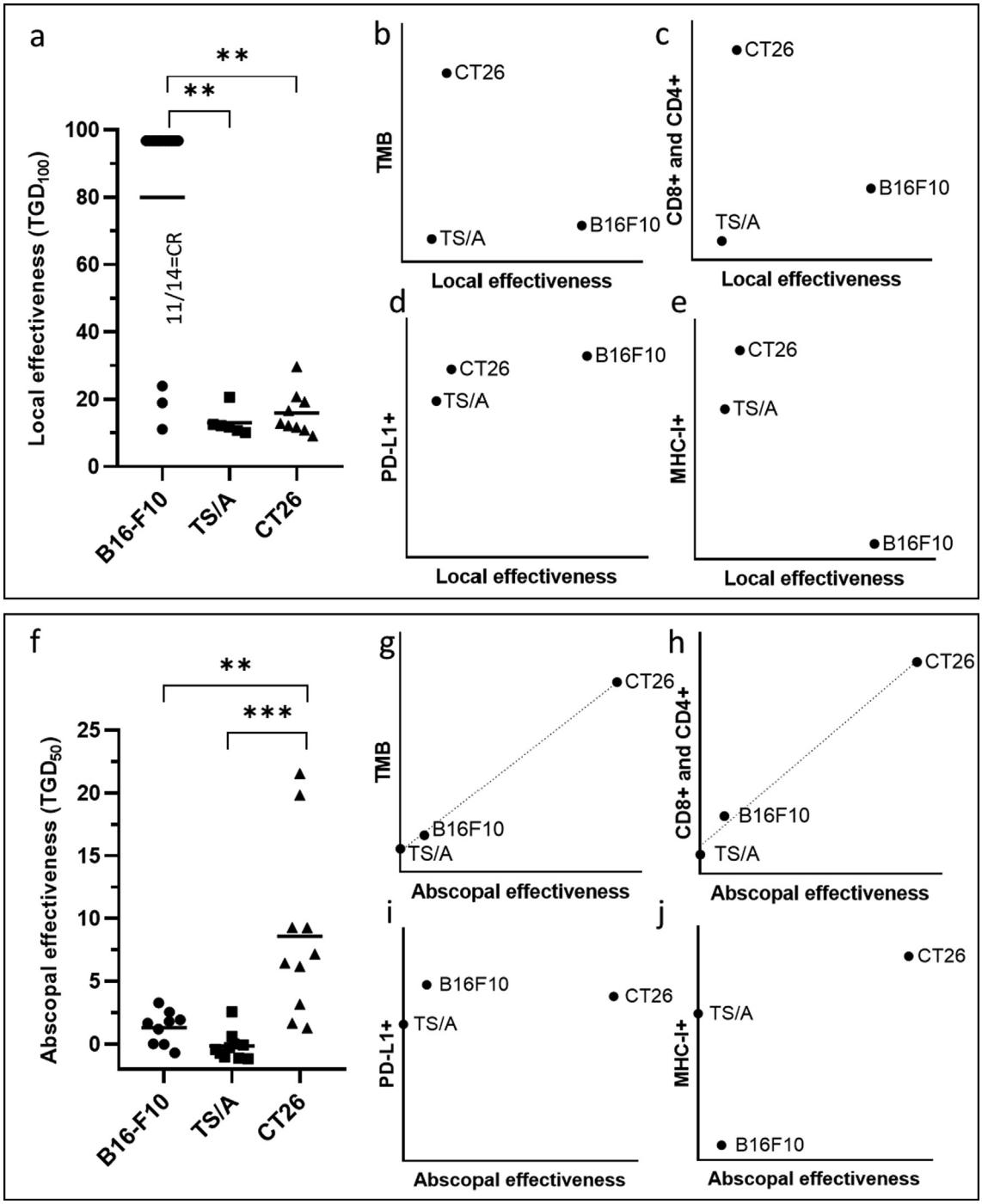

Fig 4. Association of therapeutic effectiveness (local and abscopal) of concomitant IL-12 and TNFα GET with immune profiles in B16-F10, TS/A and CT26 tumor models. Summarizing graphs for (a) local (TGD_{100}) and (f) abscopal effectiveness (TGD_{50}) for the untreated tumor. Correlation between local effectiveness and (b) tumor mutational burden (TMB), (c) infiltration of tumors by CD8+ and CD4+ immune cells, expression of (d) PD-L1 and (e) MHC-I on tumor cells. Correlation between abcsopal effectiveness and (g) tumor mutational burden, (h) infiltration of tumors by CD8+ and CD4+ immune cells, expression of (i) PD-L1 and (j) MHC-I on tumor cells. TGD_{100} and TGD_{50} drawn as individual values with mean. Correlations drawn as mean TGD_{100} or TGD_{50} plotted against TMB, mean CD8+ and CD4+ infiltration and mean PD-L1 and MHC-I expression. Simple linear regression lines indicate statistically significant correlation. (TMB) tumor mutational burden. (CR) complete response (**) $P \leq 0.01$, (***) $P \leq 0.001$.

local effectiveness of the treatment in TS/A and CT26 tumor models is lower than in B16-F10 tumors. Contrariwise, the abscopal effectiveness was detected in CT26 tumors only.

When correlating the results for local and systemic effectiveness to the tumor immune status, we hypothesized that two main requirements must be met for successful *in situ* vaccination. The first is a high tumor antigenicity, which increases with TMB [30,31] and can decrease with acquired immunosuppressive mechanisms such as MHC-I down regulation [32]. For an effective *in situ* vaccination the tumors must be mutated because a source of tumor antigens is needed, and immune cells must see their target, meaning MHC-I expression must not be hampered. Secondly, tumor microenvironment must support immune infiltration without immune suppression, *e.g.* through the expression of inhibitory immune ligands, such as PD-L1 [33]. In the present study, these hypotheses were generally confirmed. Although none of the tested

immune characteristic proved to be predictive for local effectiveness, high TMB, immune infiltration of CD4+ and CD8+ cells, and MHC-I expression proved important for achieving abscopal effectiveness.

Our results indicate that high antigenicity is a critical requirement for systemic effectiveness of *in situ* vaccination. TMB is the primary surrogate marker for neoantigens, and therefore antigenicity [30,31]. We believe that the low local and the lack of the systemic effectiveness in the TS/A tumors demonstrated in our study, could be due to the shortage of strong antigens, since the lowest TMB was determined in this tumor model. In addition, it was reported that the entire immune response against TS/A is focused on a single virus derived antigen [34,35]. Nevertheless, some other acquired immunosuppressive mechanisms could also be at work, such as PD-L1 expression, which was high in all of the tested tumor models. This is endorsed by studies using radiotherapy to induce *in situ* vaccination, where adding a systemic checkpoint inhibitors was reported to release an abscopal effect in the TS/A and also in the CT26 and B16-F10 tumors [36,37].

On the other hand, MHC-I down-regulation, can also cause low antigenicity. We believe this was demonstrated nicely in our study in B16-F10 tumor model, in which treatment was very successful locally, presumably because IL-12 GET has increased immune infiltration and expression of MHC-I through the induction of IFN-γ [38,39]. However, it was not effective in the untreated, distant tumor, even though expansion of Granzyme B positive cells in the lymph nodes was clearly demonstrated in our previous study using ELISpot [9], indicating involvement of a tumor-derived suppression in the secondary untreated tumor.

The main difference in the mechanism for local and systemic performance of *in situ* vaccination is that systemic effectiveness is exclusively due to the specific systemic immune response that is triggered in the primary tumor and has to work at the distant untreated tumor. Local effectiveness, however, is the reflection of direct cytoreductive effects of the treatment, coupled with immunological effects in the environment that is changed by the treatment. Since abscopal effect of IL-12 GET were reported in other studies using B16-F10 tumor model [40,41] and also in clinical studies in melanoma patients [42,43], we believe its lack in our study is due to the distinctive plasmid we used. Namely, our plasmid was prepared to supports paracrine secretion of IL-12 [16,44], while in most other GET studies, some IL-12 or its downstream effector IFN-γ was released systemically. This systemic release was lacking in our current study. Therefore, we are assuming that any specific immune response induced in the treated tumor was abolished in the untreated tumor by B16-F10′s intrinsic MHC-I suppression, hiding the tumor antigens and consequently lowering the antigenicity of tumor cells.

The only tumor model, in which we achieved abscopal effectiveness, was the immunologically hot CT26 tumor model, in which the systemic effects were not hindered by the lack of antigens, MHC-I suppression or low infiltration of immune cells. Additionally, in this tumor model, positive correlation in growth of treated and untreated tumors in the same mouse was detected, meaning that regression of primary tumor was positively affecting the growth of the secondary tumors and *vice versa*. However, also in this tumor model, we failed to achieve a complete local or systemic tumor control. Based on our results and other publication using this preclinical model [13,45,46], we believe that the suppression of tumor-specific immune cells through PD-L1 expression on tumor cells is responsible for the limited effectiveness in this tumor model. Consequently, using inhibition of suppression, *e.g.* PD-1/PD-L1-blocking antibodies, in combination with *in situ* vaccination, would probably be a more effective treatment in tumors that are already heavily infiltrated with immune cells.

Taken together, we have confirmed that both the abundance (high TMB) and presentation of tumor antigens (MHC-I expression) as well as the absence of immunosuppressive mechanisms are important for effective *in situ* vaccination. In the study, we have focused only on a few selected pre-treatment characteristics of tumors that could serve as predictive factors for the treatment outcome: *i.e.* TMB, infiltration of tumors with CD4+ and CD8+ immune cells and expression of PD-L1 and MHC-I on tumor cells. However, multiple other characteristics (both pre-treatment and post-treatment) could also be affecting the results; such as tumor growth kinetics, tumor vascularization, and the recruitment of suppressor cell, *e.g.* regulatory T cells (Tregs), myeloid-derived suppressor cells (MDSCs) and tumor-associated macrophages (TAMs) [11,33,47,48]. Lastly, inflammatory cytokines, including the transfected IL-12 and TNFα, could also be differentially expressed in separate tumor models. The current study therefore serves as the basis for future studies of *in situ* vaccination based approaches.

5. Conclusions

The result of the present study have highlighted the importance of choosing the right preclinical tumor model to better predict the treatment effectiveness in the clinical situation. Ideally, a range of tumor models covering the range of tumor-immune profiles found in humans should be used. Namely, even though *in situ* vaccination has potential to be effective in diverse tumor types since it utilizes tumor's own antigens, this study evidenced it is much more complicated. Our results indicate that abundance (high TMB) and the presentation (MHC-I expression) of tumor antigens is a critical requirement for systemic effectiveness of *in situ* vaccination. We have also shown that our approach may not be sufficient to overcome all the immunosuppressive mechanisms (MHC-I suppression, PD-L1 expression) in the untreated, distant metastases, justifying combinations with treatments that enable systemic relief of such immunosuppressive mechanisms. These findings have provided important indications for future development of this and similar therapeutic approaches. Furthermore, they have set the foundations for identifying the subset of tumor types that will most likely benefit from *in situ* vaccination based treatments, leading to more personalized treatments.

Funding

This work was supported by the Slovenian Research Agency under the scope of the Program P3-0003, grant number J3-8202 and J3-2528. The investment was co-financed by the Republic of Slovenia and the European Regional Development Fund (Project SmartGene.Si).

Declaration of competing interest

The authors declare that they have no known competing financial interests or personal relationships that could have appeared to influence the work reported in this paper

Appendix A. Supplementary data

Supplementary data to this article can be found online at https://doi.org/10.1016/j.bioelechem.2021.107831.

References

[1] L. Hammerich, A. Binder, J.D. Brody, In situ vaccination: Cancer immunotherapy both personalized and off-the-shelf, Mol. Oncol. 9 (2015) 1966–1981, https://doi.org/10.1016/j.molonc.2015.10.016.

[2] R.H. Pierce, J.S. Campbell, S.I. Pai, J.D. Brody, H.E.K. Kohrt, In-situ tumor vaccination: Bringing the fight to the tumor, Hum. Vaccines Immunother. 11 (2015) 1901–1909, https://doi.org/10.1080/21645515.2015.1049779.
[3] U. Kamensek, S. Kos, G. Serša, Adjuvant immunotherapy as a tool to boost effectiveness of electrochemotherapy, 2017. https://doi.org/10.1007/978-3-319-32886-7_105.
[4] K. Reynders, T. Illidge, S. Siva, J.Y. Chang, D. De Ruysscher, The abscopal effect of local radiotherapy: using immunotherapy to make a rare event clinically relevant, Cancer Treat. Rev. 41 (2015) 503–510, https://doi.org/10.1016/j.ctrv.2015.03.011.
[5] View of Combining radiotherapy and immunotherapy in definitive treatment of head and neck squamous cell carcinoma: review of current clinical trials, (n.d.). https://www.radioloncol.com/index.php/ro/article/view/3537/4783 (accessed December 30, 2020).
[6] E. Signori, S. Iurescia, E. Massi, D. Fioretti, P. Chiarella, M. De Robertis, M. Rinaldi, G. Tonon, V.M. Fazio, DNA vaccination strategies for anti-tumour effective gene therapy protocols, Cancer Immunol. Immunother. 59 (2010) 1583–1591, https://doi.org/10.1007/s00262-010-0853-x.
[7] M.-P. Rols, M. Golzio, J. Kolosnjaj-Tabi, Electric Field Based Therapies in Cancer Treatment, Cancers (Basel). 12 (2020) 3420, https://doi.org/10.3390/cancers12113420.
[8] D.A. Canton, S. Shirley, J. Wright, R. Connolly, C. Burkart, A. Mukhopadhyay, C. Twitty, K.E. Qattan, J.S. Campbell, M.H. Le, R.H. Pierce, S. Gargosky, A. Daud, A. Algazi, Melanoma treatment with intratumoral electroporation of tavokinogene telseplasmid (pIL-12, tavokinogene telseplasmid), Immunotherapy 9 (2017) 1309–1321, https://doi.org/10.2217/imt-2017-0096.
[9] U. Kamensek, M. Cemazar, U. Lampreht Tratar, K. Ursic, G. Sersa, Antitumor in situ vaccination effect of TNFα and IL-12 plasmid DNA electrotransfer in a murine melanoma model, Cancer Immunol. Immunother. (2018), https://doi.org/10.1007/s00262-018-2133-0.
[10] R. Bai, Z. Lv, D. Xu, J. Cui, Predictive biomarkers for cancer immunotherapy with immune checkpoint inhibitors, n.d. https://doi.org/10.1186/s40364-020-00209-0.
[11] S.I.S. Mosely, J.E. Prime, R.C.A. Sainson, J.-O. Koopmann, D.Y.Q. Wang, D.M. Greenawalt, M.J. Ahdesmaki, R. Leyland, S. Mullins, L. Pacelli, D. Marcus, J. Anderton, A. Watkins, J. Coates Ulrichsen, P. Brohawn, B.W. Higgs, M. McCourt, H. Jones, J.A. Harper, M. Morrow, V. Valge-Archer, R. Stewart, S.J. Dovedi, R.W. Wilkinson, Rational Selection of Syngeneic Preclinical Tumor Models for Immunotherapeutic Drug Discovery, Cancer Immunol. Res. 5 (2016) 29–41, https://doi.org/10.1158/2326-6066.cir-16-0114.
[12] W. Zhong, J.S. Myers, F. Wang, K. Wang, J. Lucas, E. Rosfjord, J. Lucas, A.T. Hooper, S. Yang, L.A. Lemon, M. Guffroy, C. May, J.R. Bienkowska, P.A. Rejto, Comparison of the molecular and cellular phenotypes of common mouse syngeneic models with human tumors, BMC Genomics 21 (2020) 1–17, https://doi.org/10.1186/s12864-019-6344-3.
[13] J.C. Castle, M. Loewer, S. Boegel, J. de Graaf, C. Bender, A.D. Tadmor, V. Boisguerin, T. Bukur, P. Sorn, C. Paret, M. Diken, S. Kreiter, Ö. Türeci, U. Sahin, Immunomic, genomic and transcriptomic characterization of CT26 colorectal carcinoma, BMC Genomics 15 (2014), https://doi.org/10.1186/1471-2164-15-190.
[14] M.G. Lechner, S.S. Karimi, K. Barry-Holson, T.E. Angell, K.A. Murphy, C.H. Church, J.R. Ohlfest, P. Hu, A.L. Epstein, Immunogenicity of murine solid tumor models as a defining feature of in vivo behavior and response to immunotherapy, n.d. https://doi.org/10.1097/01.cji.0000436722.46675.4a.
[15] C. De Giovanni, G. Nicoletti, L. Landuzzi, A. Palladini, P.L. Lollini, P. Nanni, Bioprofiling TS/A murine mammary cancer for a functional precision experimental model, Cancers (Basel) 11 (2019), https://doi.org/10.3390/cancers11121889.
[16] U. Kamensek, N. Tesic, G. Sersa, S. Kos, M. Cemazar, Tailor-made fibroblast-specific and antibiotic-free interleukin 12 plasmid for gene electrotransfer-mediated cancer immunotherapy, Plasmid 89 (2017) 9–15, https://doi.org/10.1016/j.plasmid.2016.11.004.
[17] P. Nanni, C. Degiovanni, P.L. Lollini, G. Nicoletti, G. Prodi, Ts/A - A New Metastasizing Cell-Line from A Balb/C Spontaneous Mammary Adenocarcinoma, Clin. Exp. Metastasis 1 (1983) 373–380.
[18] J.C. Castle, M. Loewer, S. Boegel, A.D. Tadmor, V. Boisguerin, J. De Graaf, C. Paret, M. Diken, S. Kreiter, Ö. Türeci, U. Sahin, Mutated tumor alleles are expressed according to their DNA frequency, Sci. Rep. 4 (2014), https://doi.org/10.1038/srep04743.
[19] M. Stimac, U. Kamensek, M. Cemazar, S. Kranjc, A. Coer, G. Sersa, Tumor radiosensitization by gene therapy against endoglin, Cancer Gene Ther. 23 (2016), https://doi.org/10.1038/cgt.2016.20.
[20] A. Groselj, S. Kranjc, M. Bosnjak, M. Krzan, T. Kosjek, A. Prevc, M. Cemazar, G. Sersa, Vascularization of the tumours affects the pharmacokinetics of bleomycin and the effectiveness of electrochemotherapy, Basic Clin. Pharmacol. Toxicol. 123 (2018) 247–256, https://doi.org/10.1111/bcpt.13012.
[21] B. Seliger, U. Wollscheid, F. Momburg, T. Blankenstein, C. Huber, M. Delbrück, Characterization of the Major Histocompatibility Complex Class I Deficiencies in B16 Melanoma Cells 1, 2001.
[22] C. Lennicke, J. Rahn, J. Bukur, F. Hochgräfe, L.A. Wessjohann, R. Lichtenfels, B. Seliger, Modulation of MHC class I surface expression in B16F10 melanoma cells by methylseleninic acid, Oncoimmunology 6 (2017), https://doi.org/10.1080/2162402X.2016.1259049.
[23] U. Kamensek, G. Sersa, M. Cemazar, Evaluation of p21 promoter for interleukin 12 radiation induced transcriptional targeting in a mouse tumor model, Mol. Cancer 12 (2013) 136.
[24] M. Savarin, U. Kamensek, M. Cemazar, R. Heller, G. Sersa, Electrotransfer of plasmid DNA radiosensitizes B16F10 tumors through activation of immune response, Radiol. Oncol. 51 (2017), https://doi.org/10.1515/raon-2017-0011.
[25] J. Diamond, K. Pilones, J. Aryankalayil, R. Vatner, S. Formenti, S. Demaria, Radiotherapy induces responsiveness of a resistant mammary carcinoma to PD-1 blockade, 2014. https://doi.org/10.1186/2051-1426-2-S3-P159.
[26] B. Meléndez, C. Van Campenhout, S. Rorive, M. Remmelink, I. Salmon, N. D'Haene, Methods of measurement for tumor mutational burden in tumor tissue, Transl. Lung Cancer Res. 7 (2018) 661–667, https://doi.org/10.21037/tlcr.2018.08.02.
[27] C.U. Blank, J.B. Haanen, A. Ribas, T.N. Schumacher, CANCER IMMUNOLOGY. The "cancer immunogram", Science 352 (80) (2016) 658–660, https://doi.org/10.1126/science.aaf2834.
[28] N. Meena, P. Mathur, K.M. Medicherla, P. Suravajhala, A Bioinformatics Pipeline for Whole Exome Sequencing: Overview of the Processing and Steps from Raw Data to Downstream Analysis, n.d. https://doi.org/10.1101/201145.
[29] T.D. Andrews, B. Whittle, M.A. Field, B. Balakishnan, Y. Zhang, Y. Shao, V. Cho, M. Kirk, M. Singh, Y. Xia, J. Hager, S. Winslade, G. Sjollema, B. Beutler, A. Enders, C.C. Goodnow, Massively parallel sequencing of the mouse exome to accurately identify rare, induced mutations: an immediate source for thousands of new mouse models, Open Biol. 2 (2012), https://doi.org/10.1098/rsob.120061 120061.
[30] C. Heydt, J. Rehker, R. Pappesch, T. Buhl, M. Ball, U. Siebolts, A. Haak, P. Lohneis, R. Büttner, A.M. Hillmer, S. Merkelbach-Bruse, Analysis of tumor mutational burden: correlation of five large gene panels with whole exome sequencing, Sci. Rep. 10 (2020), https://doi.org/10.1038/s41598-020-68394-4.
[31] P. Bonaventura, T. Shekarian, V. Alcazer, J. Valladeau-Guilemond, S. Valsesia-Wittmann, S. Amigorena, C. Caux, S. Depil, Cold tumors: A therapeutic challenge for immunotherapy, Front. Immunol. 10 (2019) 168, https://doi.org/10.3389/fimmu.2019.00168.
[32] F. Garrido, N. Aptsiauri, E.M. Doorduijn, A.M. Garcia Lora, T. van Hall, The urgent need to recover MHC class I in cancers for effective immunotherapy, Curr. Opin. Immunol. 39 (2016) 44–51, https://doi.org/10.1016/j.coi.2015.12.007.
[33] G.W. Tormoen, M.R. Crittenden, M.J. Gough, Role of the immunosuppressive microenvironment in immunotherapy, Adv. Radiat. Oncol. 3 (2018) 520–526, https://doi.org/10.1016/j.adro.2018.08.018.
[34] A. Rosato, S.D. Santa, A. Zoso, S. Giacomelli, G. Milan, B. Macino, V. Tosello, P. Dellabona, P. Lollini, C. De Giovanni, P. Zanovello, The Cytotoxic T-Lymphocyte Response against a Poorly Immunogenic Mammary Adenocarcinoma Is Focused on a Single Immunodominant Class I Epitope Derived from the gp70 Env Product of an, Endogenous Retrovirus 1 (2003) 2158–2163.
[35] C. Vanpouille-Box, J.M. Diamond, K.A. Pilones, J. Zavadil, J.S. Babb, S.C. Formenti, M.H. Barcellos-Hoff, S. Demaria, TGFβ is a master regulator of radiation therapy-induced antitumor immunity, Cancer Res. 75 (2015) 2232–2242, https://doi.org/10.1158/0008-5472.CAN-14-3511.
[36] W. Ngwa, O. Credit Irabor, J.D. Schoenfeld, J. Hesser, S. Demaria, S.C. Formenti, Using immunotherapy to boost the abscopal effect, n.d. https://doi.org/10.1038/nrc.2018.6.
[37] R. Marconi, S. Strolin, G. Bossi, L. Strigari, A meta-analysis of the abscopal effect in preclinical models: Is the biologically effective dose a relevant physical trigger?, 2017. https://doi.org/10.1371/journal.pone.0171559.
[38] G. Shi, C. Edelblute, S. Arpag, C. Lundberg, R. Heller, IL-12 gene electrotransfer triggers a change in immune response within mouse tumors, Cancers (Basel) 10 (2018), https://doi.org/10.3390/cancers10120498.
[39] W. Su, T. Ito, T. Oyama, T. Kitagawa, T. Yamori, H. Fujiwara, H. Matsuda, The direct effect of IL-12 on tumor cells: IL-12 acts directly on tumor cells to activate NF-κb and enhance IFN-γ-mediated STAT1 phosphorylation, Biochem. Biophys. Res. Commun. 280 (2001) 503–512, https://doi.org/10.1006/bbrc.2000.4150.
[40] A. Mukhopadhyay, J. Wright, S. Shirley, D.A. Canton, C. Burkart, R.J. Connolly, J. S. Campbell, R.H. Pierce, Characterization of abscopal effects of intratumoral electroporation-mediated IL-12 gene therapy, Gene Ther. 26 (2019), https://doi.org/10.1038/s41434-018-0044-5.
[41] C. Burkart, A. Mukhopadhyay, S.A. Shirley, R.J. Connolly, J.H. Wright, A. Bahrami, J.S. Campbell, R.H. Pierce, D.A. Canton, Improving therapeutic efficacy of IL-12 intratumoral gene electrotransfer through novel plasmid design and modified parameters, Gene Ther. 25 (2018) 93–103, https://doi.org/10.1038/s41434-018-0006-y.
[42] A.I. Daud, R.C. DeConti, S. Andrews, P. Urbas, A.I. Riker, V.K. Sondak, P.N. Munster, D.M. Sullivan, K.E. Ugen, J.L. Messina, R. Heller, Phase I Trial of Interleukin-12 Plasmid Electroporation in Patients With Metastatic Melanoma, J. Clin. Oncol. 26 (2008) 5896–5903, https://doi.org/10.1200/Jco.2007.15.6794.
[43] A. Algazi, S. Bhatia, S. Agarwala, M. Molina, K. Lewis, M. Faries, L. Fong, L.P. Levine, M. Franco, A. Oglesby, C. Ballesteros-Merino, C.B. Bifulco, B.A. Fox, D. Bannavong, R. Talia, E. Browning, M.H. Le, R.H. Pierce, S. Gargosky, K.K. Tsai, C. Twitty, A.I. Daud, Intratumoral delivery of tavokinogene telseplasmid yields systemic immune responses in metastatic melanoma patients, Ann. Oncol. 31 (2020) 532–540, https://doi.org/10.1016/j.annonc.2019.12.008.
[44] S. Kos, N. Tesic, U. Kamensek, T. Blagus, M. Cemazar, S. Kranjc, J. Lavrencak, G. Sersa, Improved Specificity of Gene Electrotransfer to Skin Using pDNA Under the Control of Collagen Tissue-Specific Promoter, J Membr Biol. (2015), https://doi.org/10.1007/s00232-015-9799-4.
[45] E. Fiegle, D. Doleschel, S. Koletnik, A. Rix, R. Weiskirchen, E. Borkham-Kamphorst, F. Kiessling, W. Lederle, Dual CTLA-4 and PD-L1 Blockade Inhibits Tumor Growth and Liver Metastasis in a Highly Aggressive Orthotopic Mouse

Model of Colon Cancer, Neoplasia (United States) 21 (2019) 932–944, https://doi.org/10.1016/j.neo.2019.07.006.
[46] J. Lau, J. Cheung, A. Navarro, S. Lianoglou, B. Haley, K. Totpal, L. Sanders, H. Koeppen, P. Caplazi, J. Mcbride, H. Chiu, R. Hong, J. Grogan, V. Javinal, R. Yauch, B. Irving, M. Belvin, I. Mellman, J.M. Kim, M. Schmidt, ARTICLE Tumour and host cell PD-L1 is required to mediate suppression of anti-tumour immunity in mice, Nat. Commun. (2017), https://doi.org/10.1038/ncomms14572.
[47] M.V. Guerin, V. Finisguerra, B.J. Van den Eynde, N. Bercovici, A. Trautmann, Preclinical murine tumor models: A structural and functional perspective, Elife 9 (2020), https://doi.org/10.7554/eLife.50740.
[48] S. Mesojednik, D. Pavlin, G. Sersa, A. Coer, S. Kranjc, A. Grosel, G. Tevz, M. Cemazar, The effect of the histological properties of tumors on transfection efficiency of electrically assisted gene delivery to solid tumors in mice, Gene Ther. 14 (2007) 1261–1269, https://doi.org/10.1038/sj.gt.3302989.